



US 20090226361A1

(19) **United States**

(12) **Patent Application Publication**  
**Campos-Delgado et al.**

(10) **Pub. No.: US 2009/0226361 A1**

(43) **Pub. Date: Sep. 10, 2009**

(54) **CVD-GROWN GRAPHITE NANORIBBONS**

(21) Appl. No.: **12/042,544**

(76) Inventors: **Jessica Campos-Delgado**, San Luis Potosi (MX); **Mildred S. Dresselhaus**, Cambridge, MA (US); **Morinobu Endo**, Nagano-shi (JP); **Edgar E. Gracia-Espino**, San Luis Potosi (MX); **Xiaoting Jia**, Cambridge, MA (US); **Jose Manuel Romo-Herrera**, San Luis Potosi (MX); **Humberto Terrones**, San Luis Potosi (MX); **Mauricio Terrones**, San Luis Potosi (MX)

(22) Filed: **Mar. 5, 2008**

**Publication Classification**

(51) **Int. Cl.**  
**D01F 9/12** (2006.01)

(52) **U.S. Cl.** ..... **423/447.2; 423/447.1**

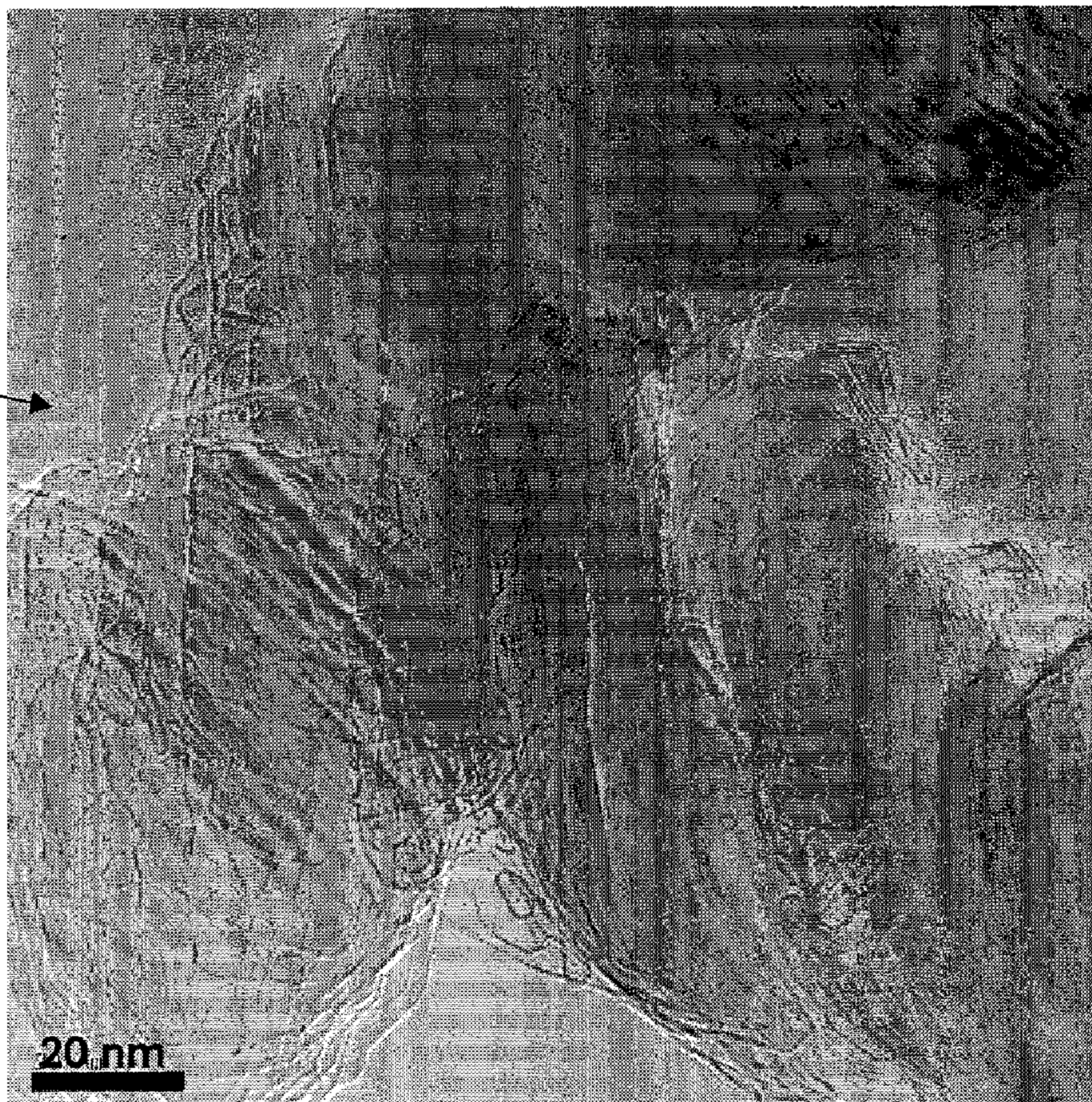
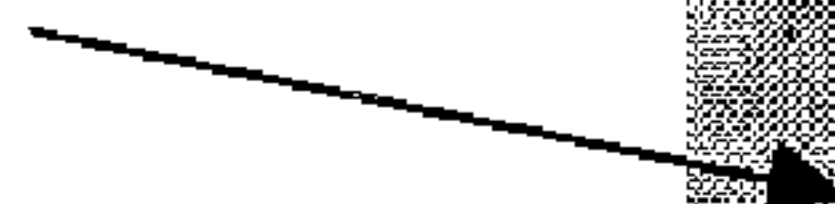
(57) **ABSTRACT**

The nanoribbon structure includes a plurality of thin graphite ribbons having long and highly crystalline structure. A voltage is applied across the length of the thin graphite ribbons to cause current flow so as to increase crystallinity as well as establishing interplanar stacking order and well-defined graphene edges of the thin graphite ribbons.

Correspondence Address:

**GAUTHIER & CONNORS, LLP**  
**225 FRANKLIN STREET, SUITE 2300**  
**BOSTON, MA 02110 (US)**

**2**



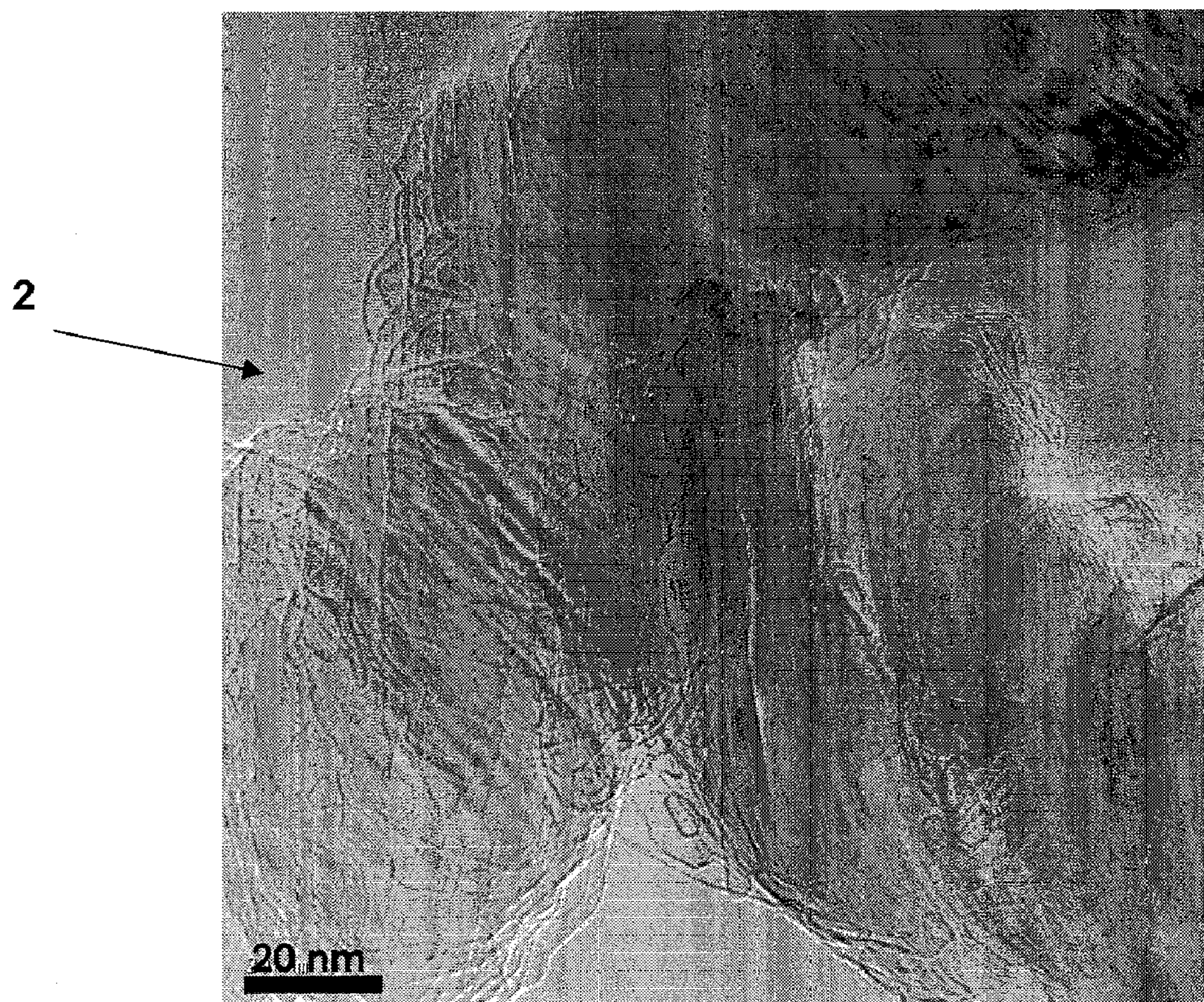


FIG. 1A

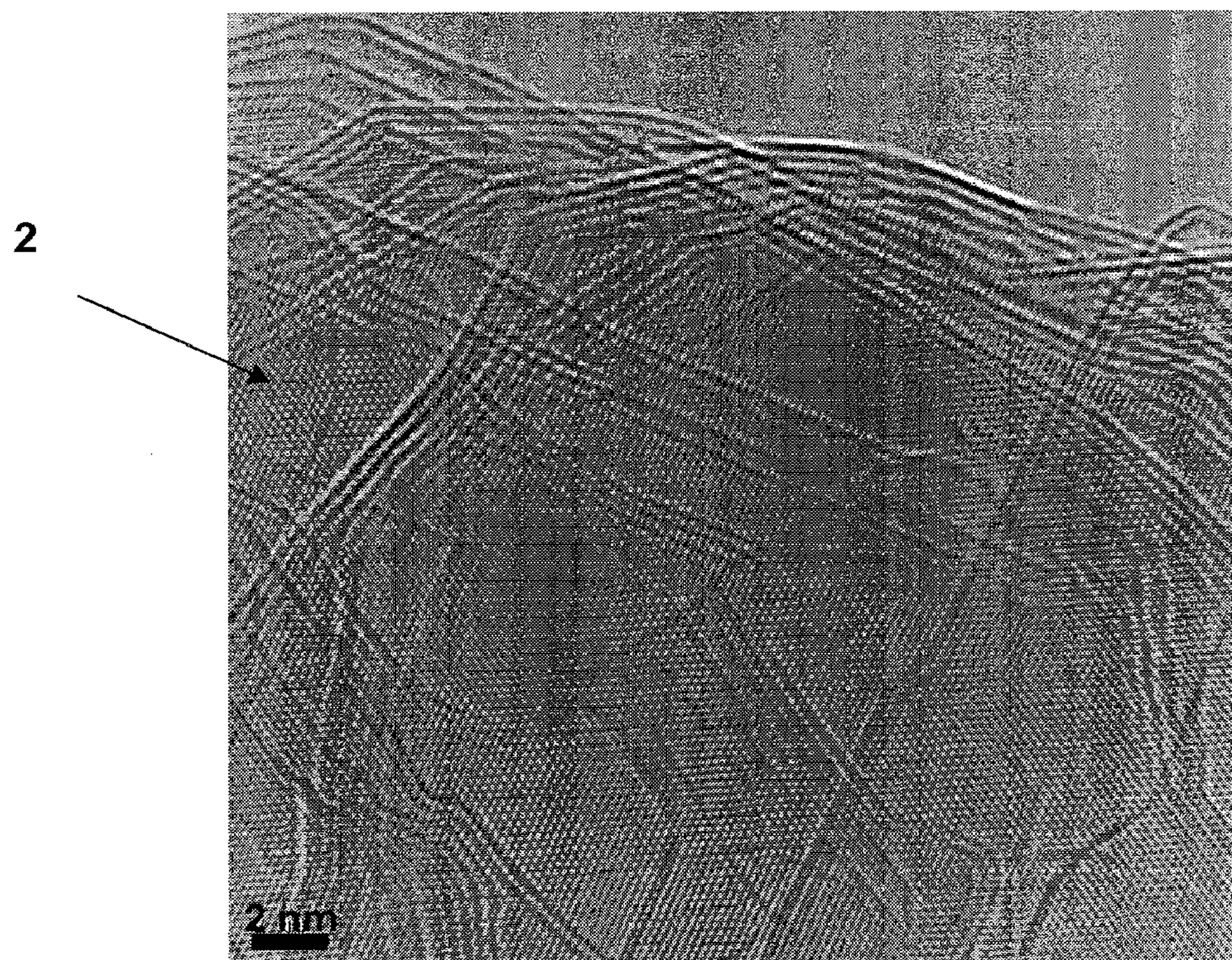


FIG. 1B

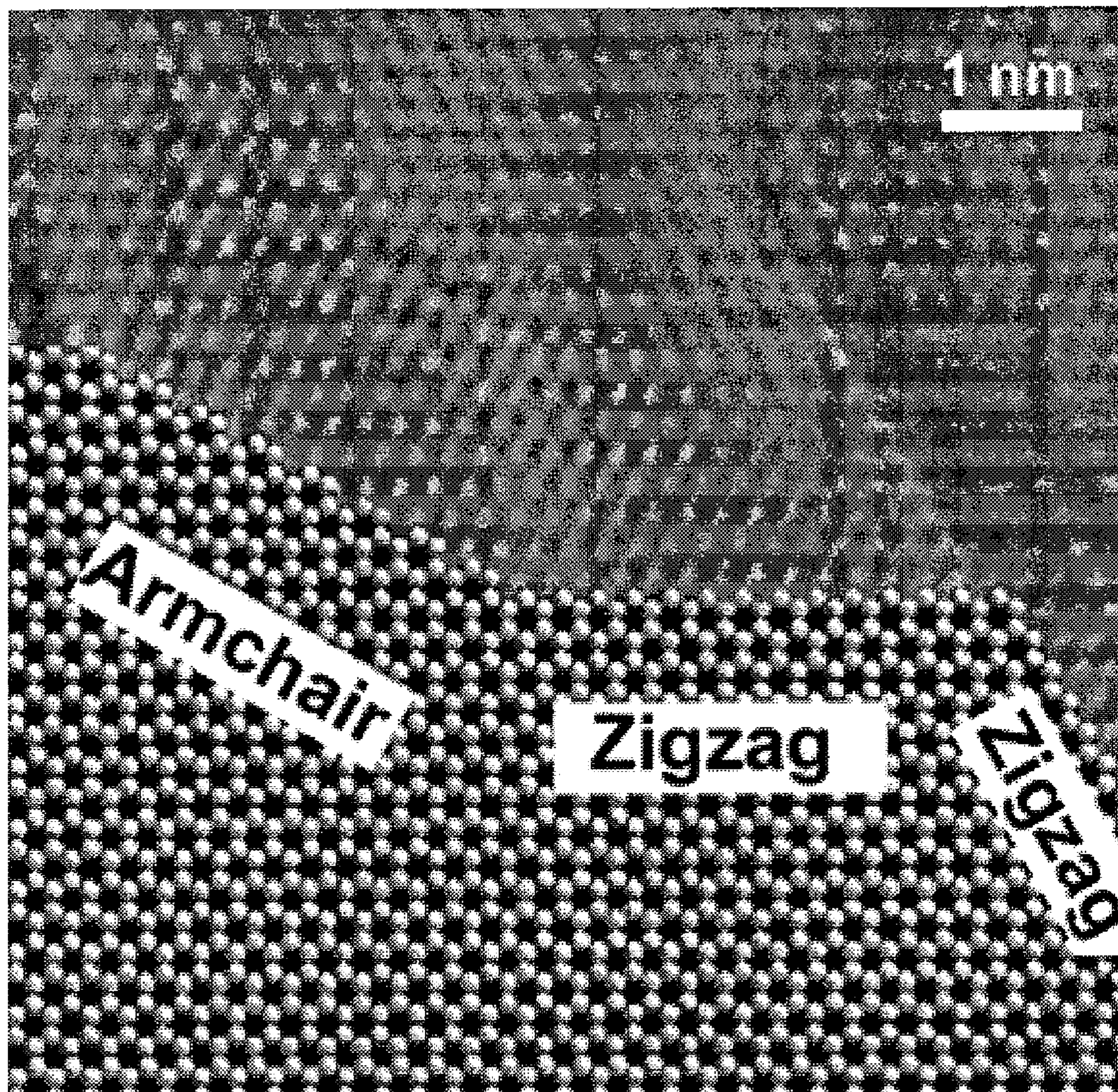


FIG. 1C

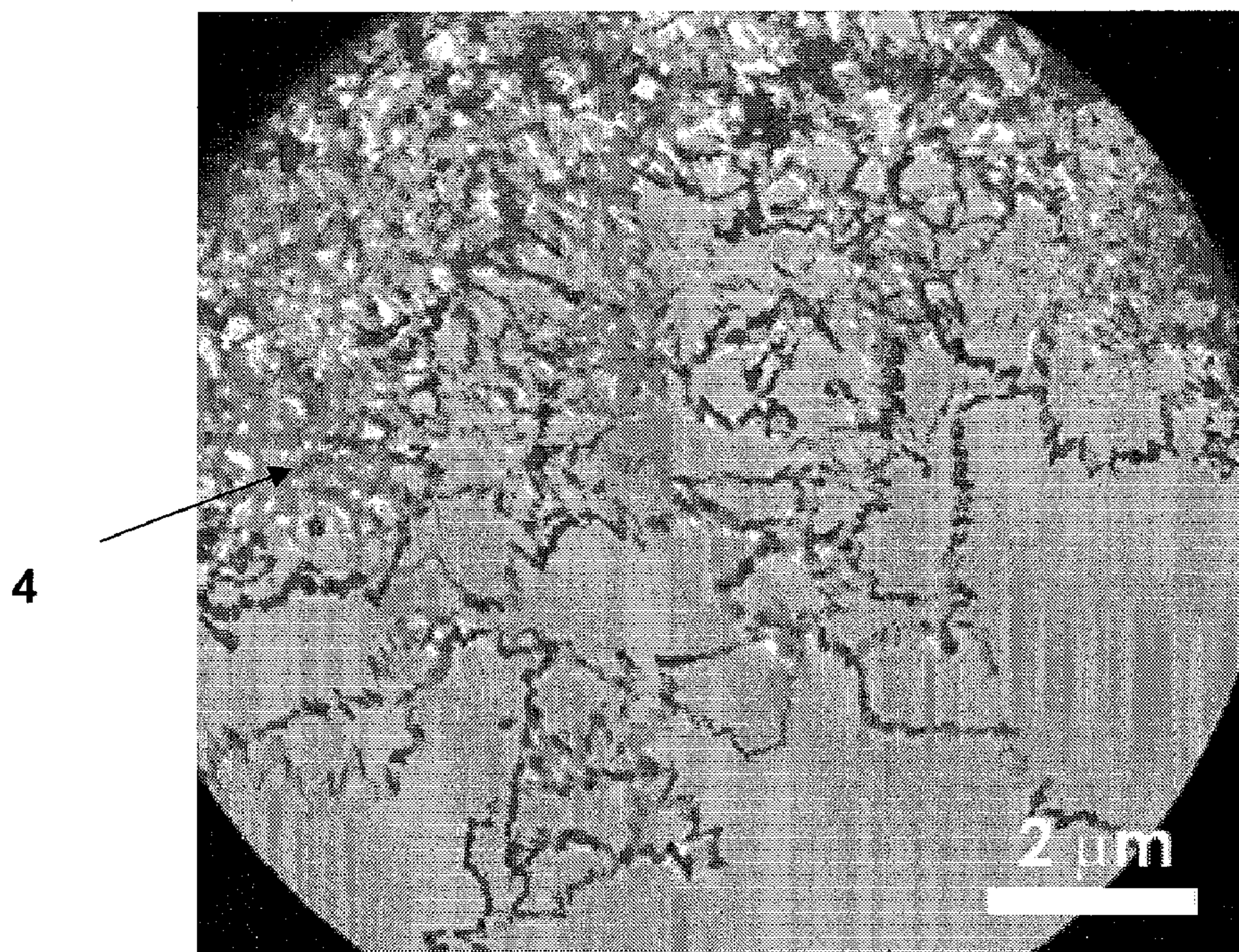


FIG. 2A

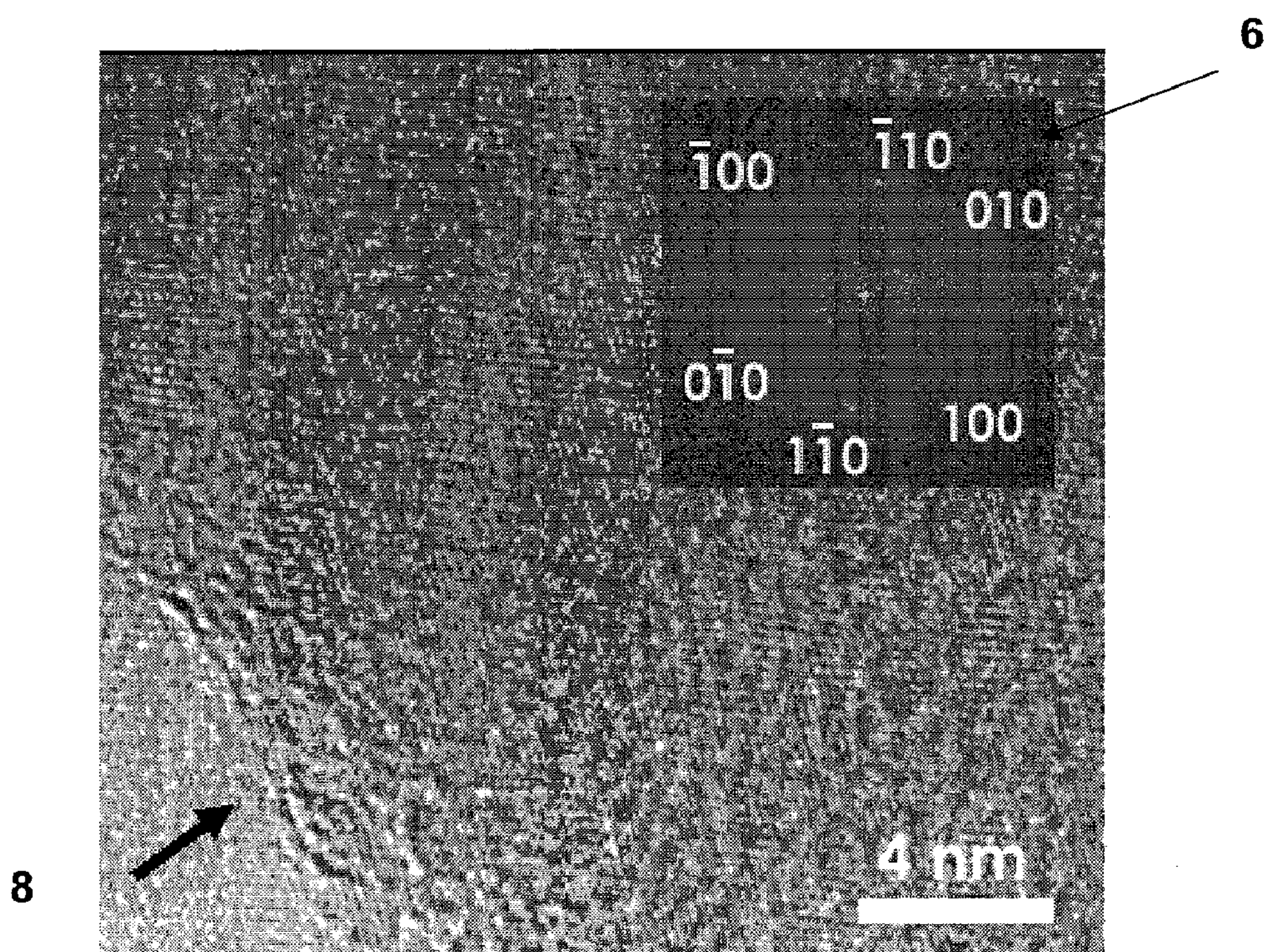


FIG. 2B

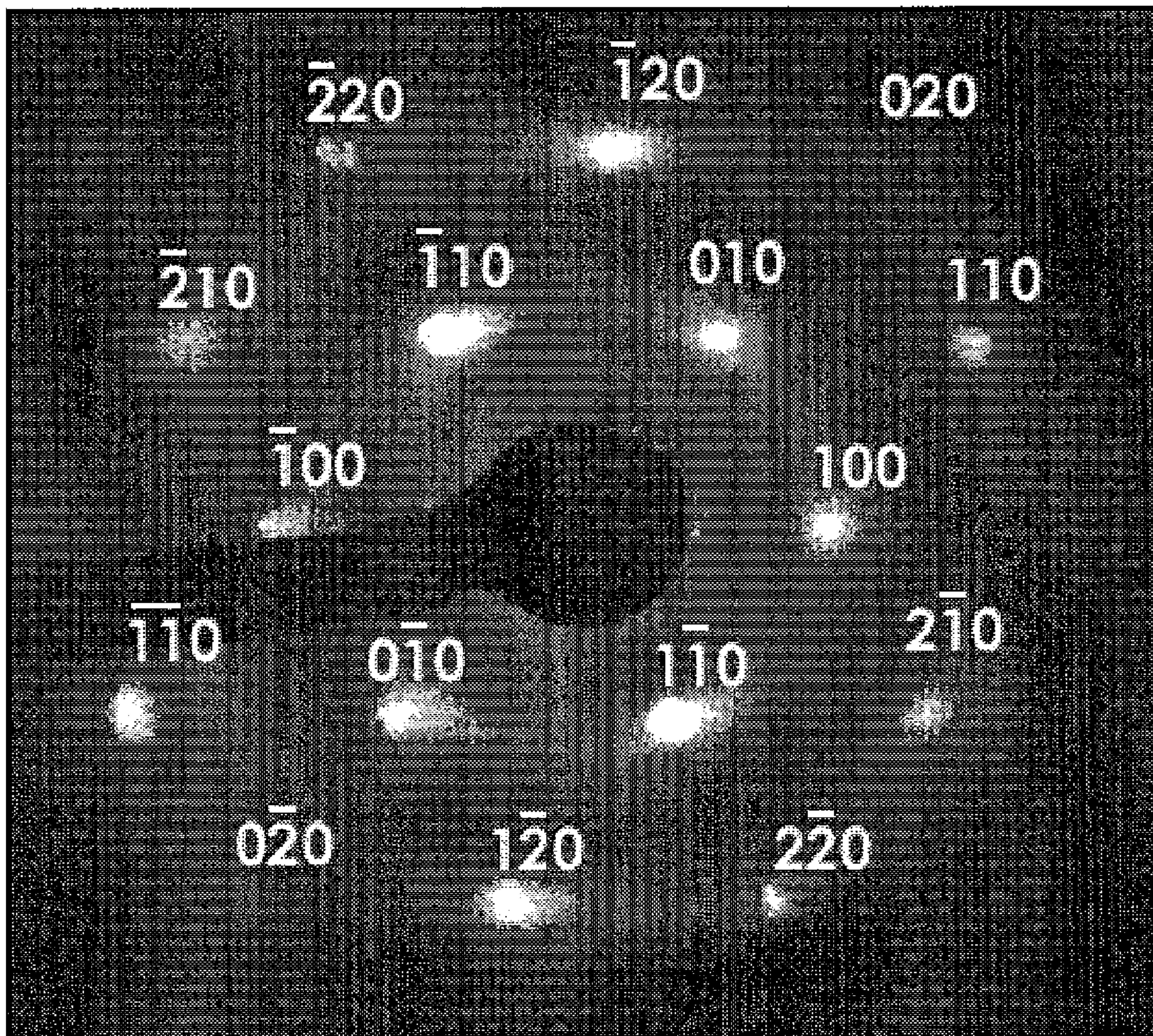


FIG. 2C

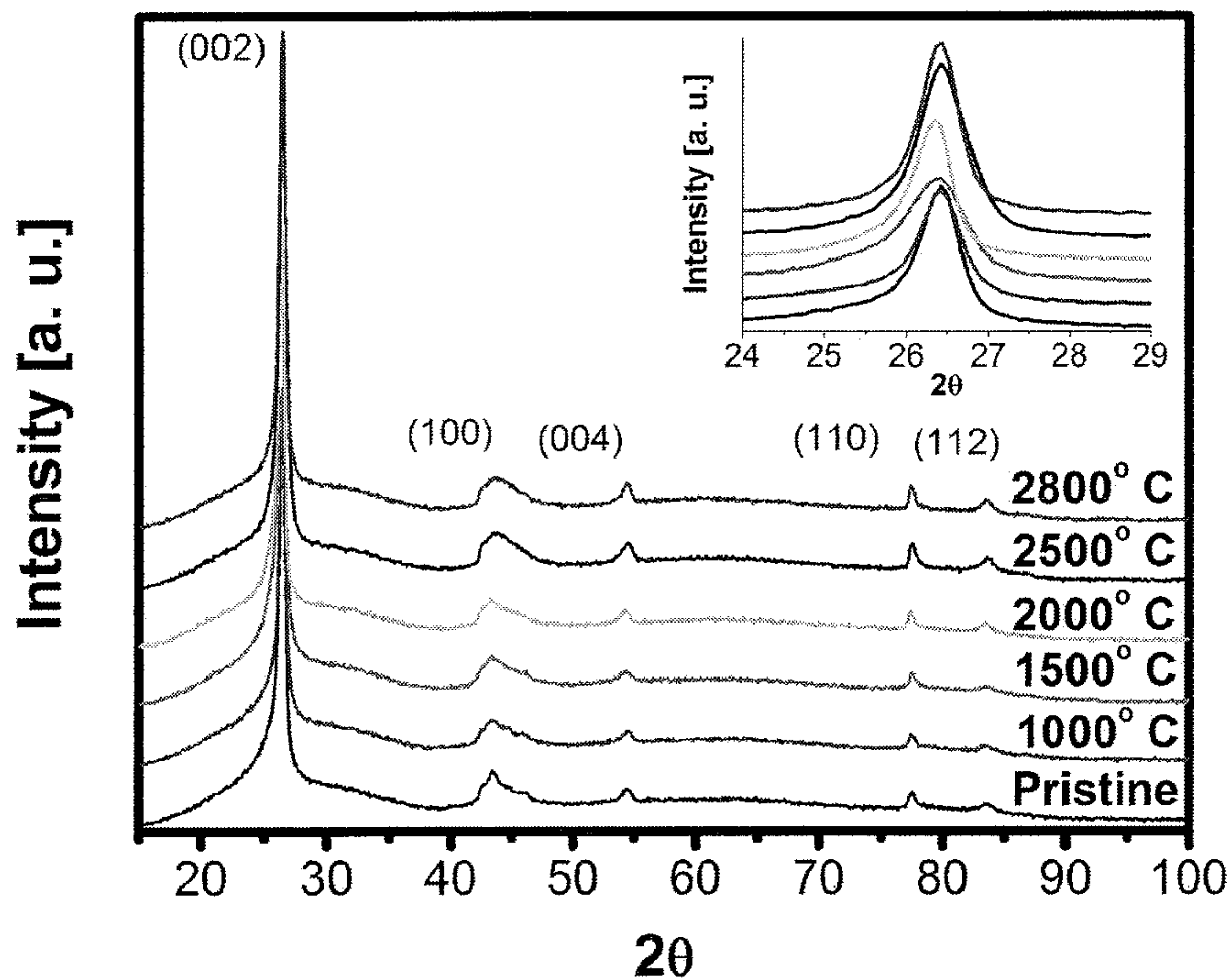


FIG. 3A

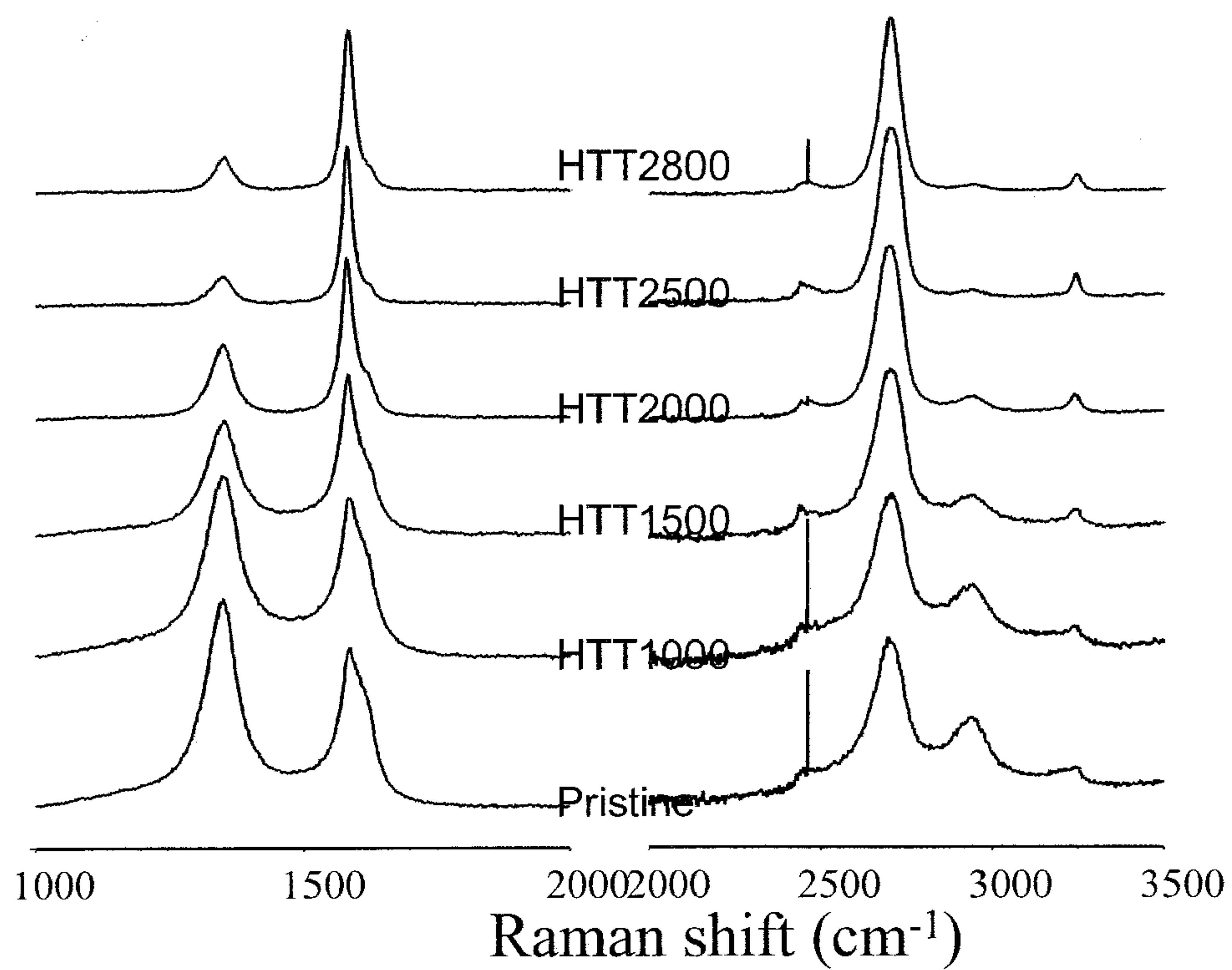


FIG. 3B

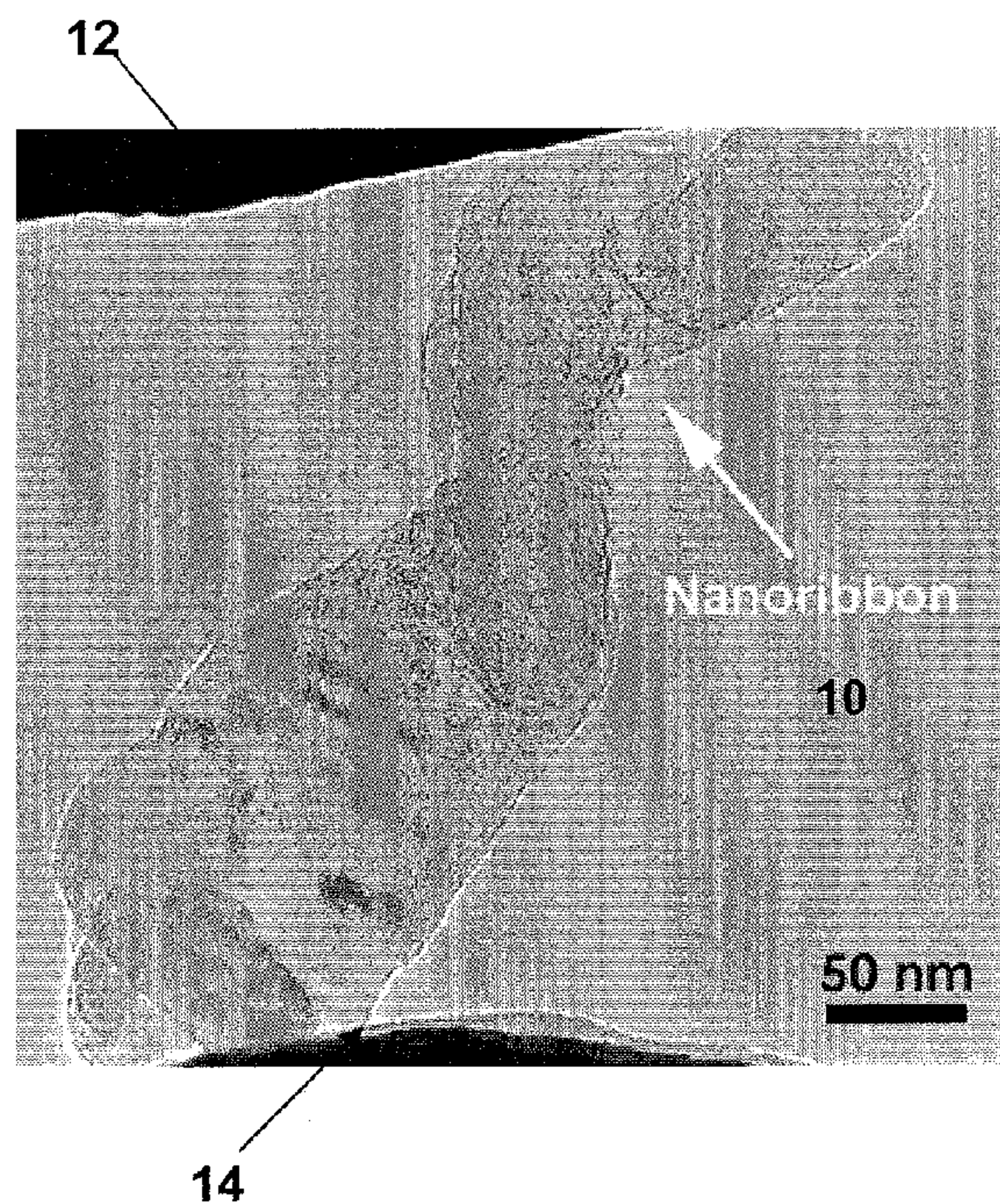


FIG. 4A

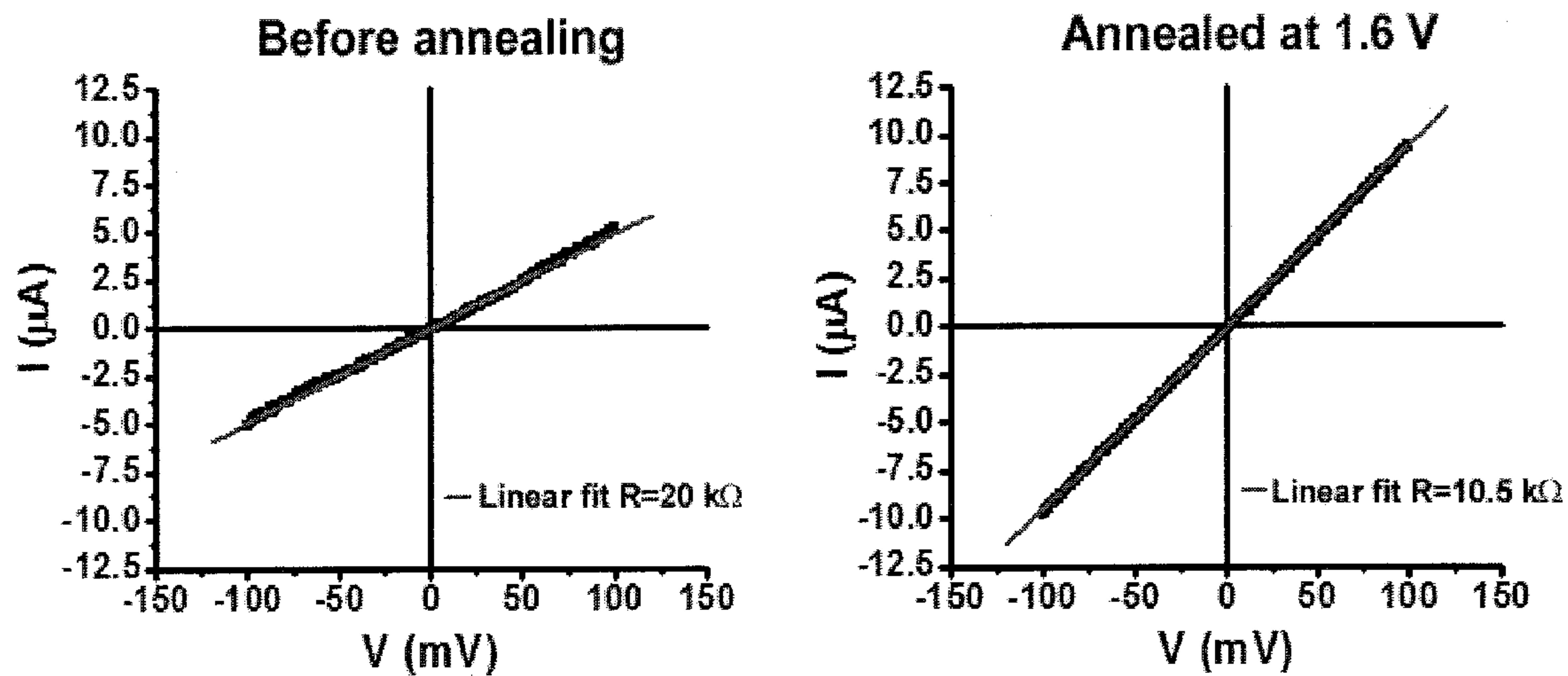


FIG. 4B

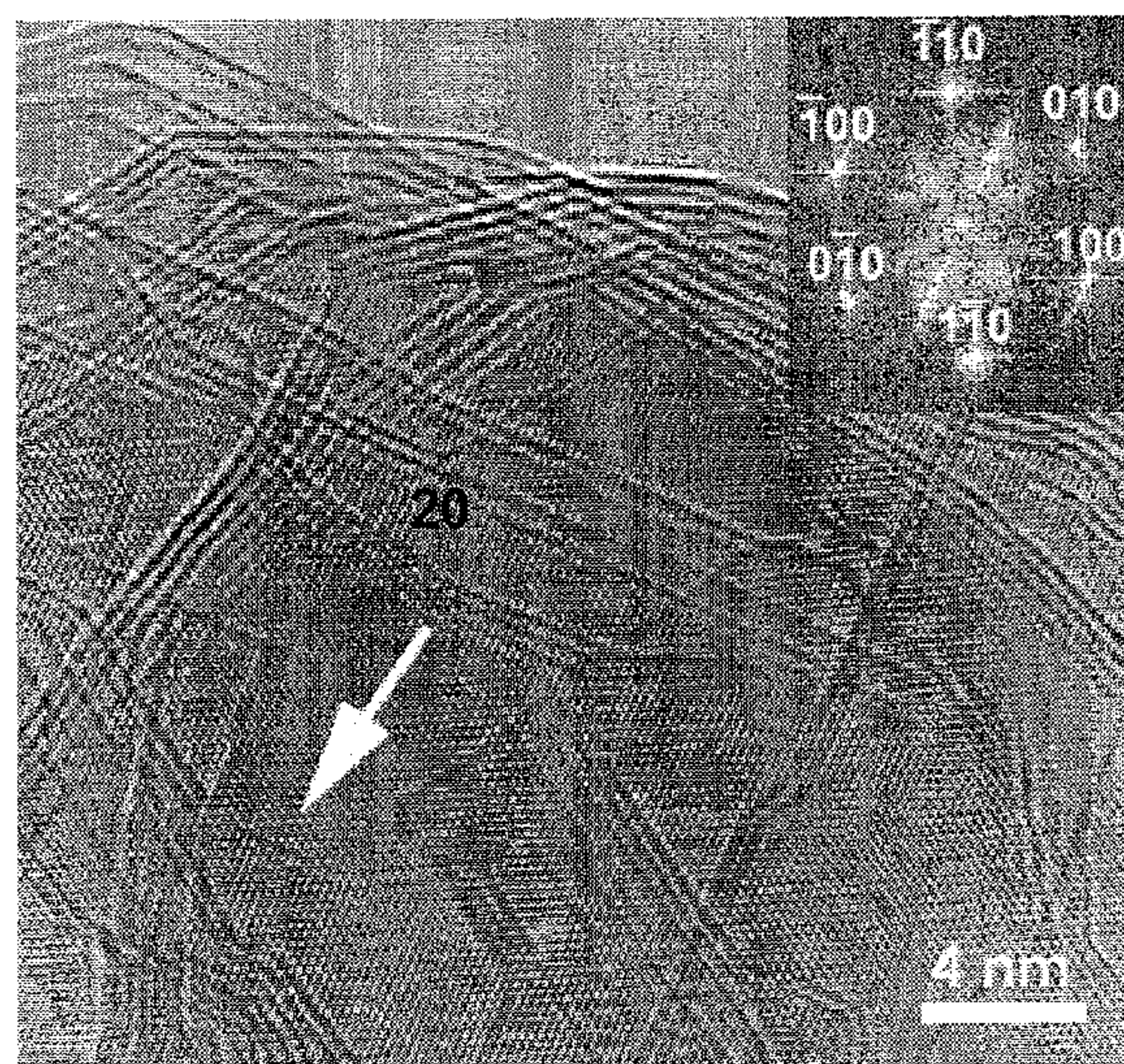


FIG. 4C

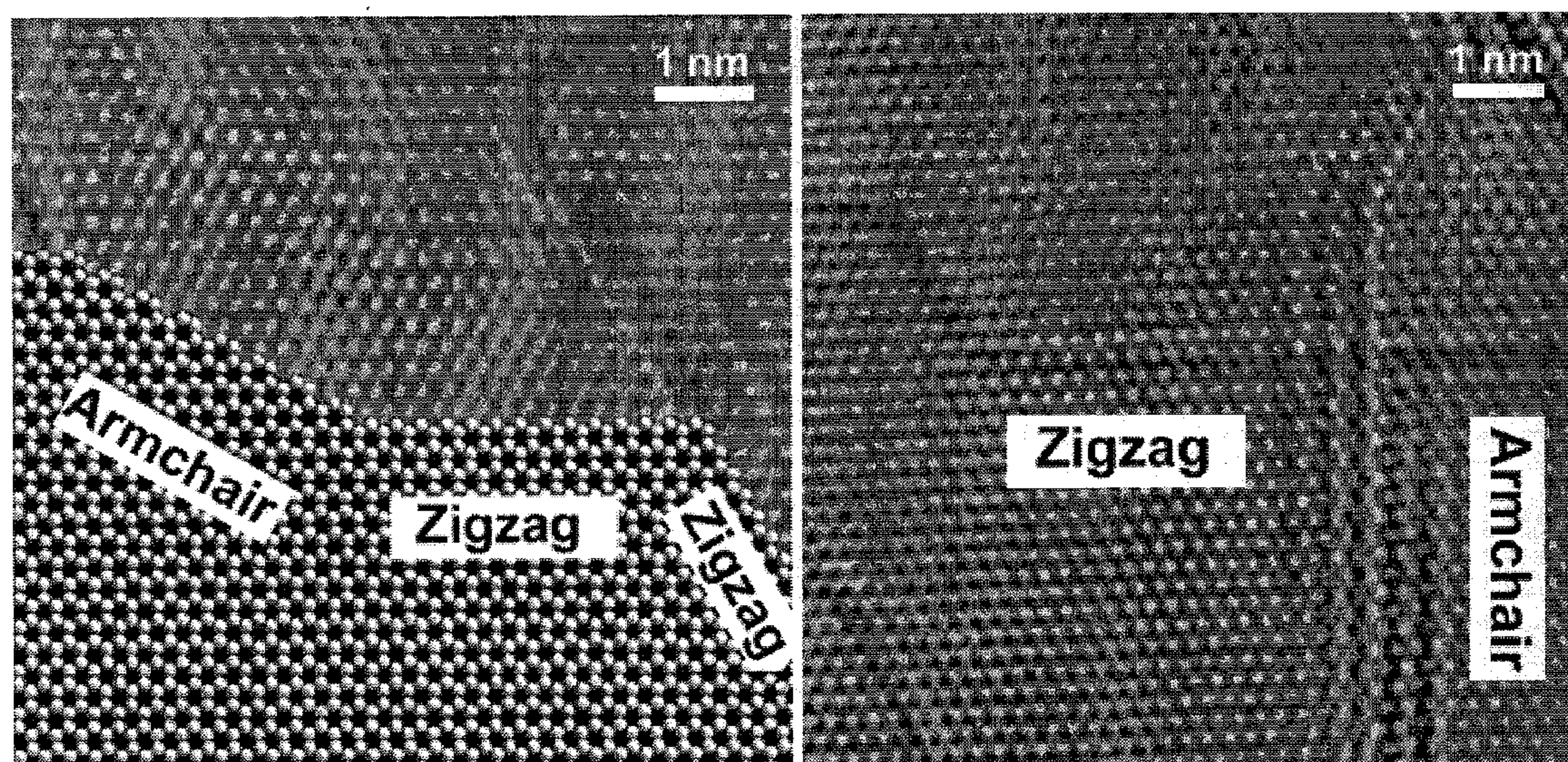
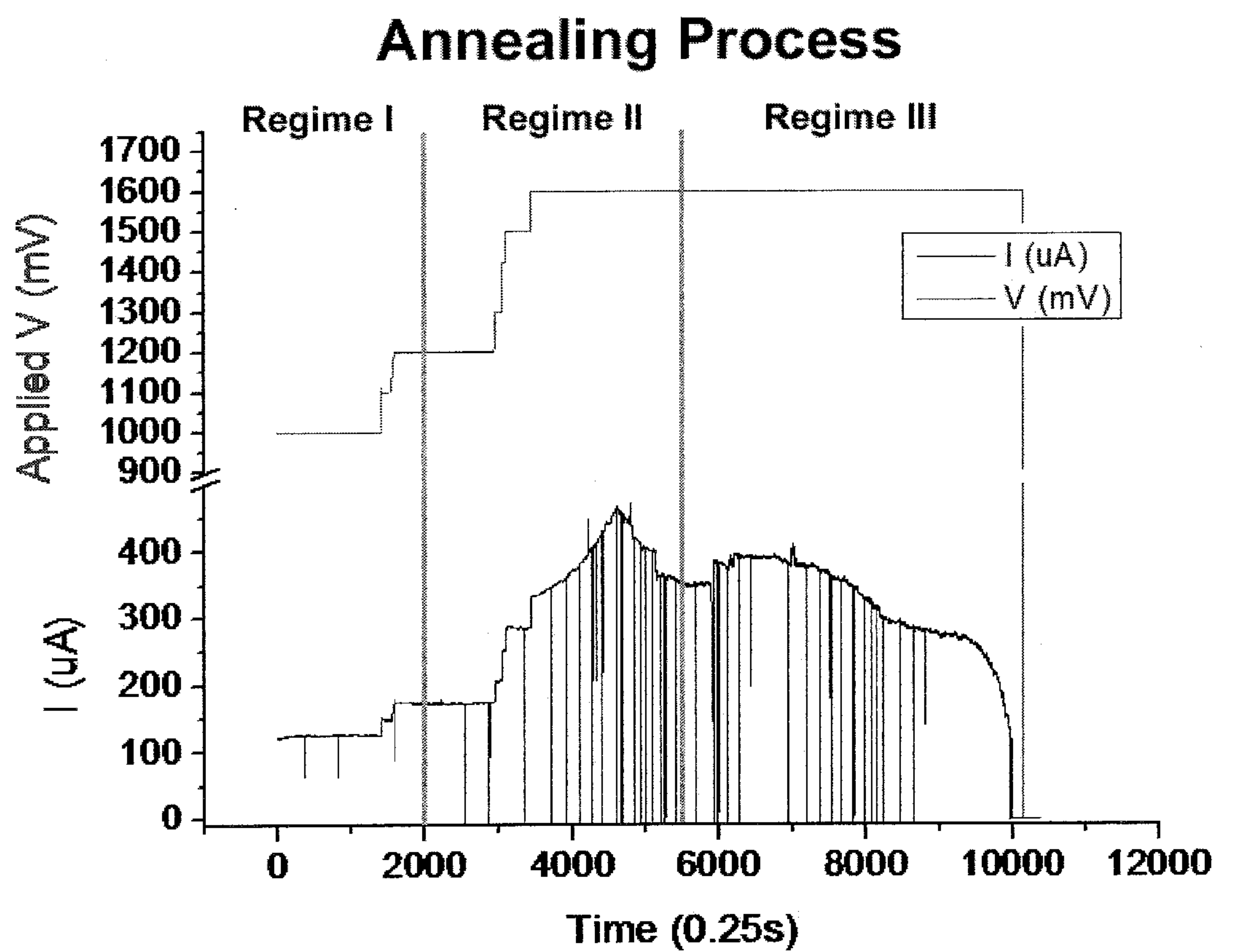


FIG. 4D



\*Each vertical line is a linear I-V sweep during annealing

FIG. 5

## CVD-GROWN GRAPHITE NANORIBBONS

### BACKGROUND OF THE INVENTION

**[0001]** The invention relates to the field of nanoribbons, and in particular to the possibility of synthesizing bulk amounts of graphene nanoribbons.

**[0002]** Following the discovery of  $C_{60}$  and its bulk production, nanoscale carbon science emerged, and other fullerene-like carbons, such as nanotubes, started to attract the attention of numerous researchers due to their fascinating physico-chemical properties. Subsequently, new experimental approaches have led to the synthesis of graphitic nanocones and nanodiscs, as well as nanohorns and toroidal structures. These results have also motivated theoretical studies on novel forms of carbon such as Schwartzites, toroids, fullerenes, nanotubes and graphene nanoribbons. In particular, graphene nanoribbons have been predicted to be metallic if their edges exhibit a zigzag morphology, whereas armchair edges can give rise to either semiconducting or metallic transport. This theoretical work has motivated the synthesis of individual graphene sheets and nanoribbons.

### SUMMARY OF THE INVENTION

**[0003]** According to one aspect of the invention, there is provided a bulk nanoribbon structure. The bulk nanoribbon structure includes a plurality of thin graphite ribbons having long and highly crystalline ribbons. A voltage is applied across the length of the thin graphite ribbons to cause current flow so as to increase crystallinity as well as establishing interplanar stacking order and well-defined graphene edges of the thin graphite ribbons.

**[0004]** According to another aspect of the invention, there is provided a method of forming bulk nanoribbon structures. The method includes forming a plurality of thin graphite ribbons having long and highly crystalline ribbons. In addition, the method includes annealing the thin graphite ribbons using Joule heating by applying a voltage across the length of the thin graphite ribbons to cause current flow so as to produce heat that increases crystallinity as well as establishing interplanar stacking order and well-defined graphene edges of the thin graphite ribbons. Finally thermal (static) heat treatments could also be applied to the nanoribbons up to  $2800^{\circ}\text{C}$ . in order to modify the structure and properties of the ribbons.

### BRIEF DESCRIPTION OF THE DRAWINGS

**[0005]** FIGS. 1A-1C are SEM images illustrating graphene nanoribbons formed in accordance with the invention;

**[0006]** FIGS. 2A-2C are TEM and HRTEM images illustrating graphene nanoribbons formed in accordance with the invention;

**[0007]** FIG. 3A-3B are graphs illustrating X-ray powder diffraction patterns and Raman spectra of the nanoribbons formed in accordance with the invention;

**[0008]** FIGS. 4A-4D are HRTEM images, diagrams and graphical results of a nanoribbon before and after Joule heating; and

**[0009]** FIG. 5 is a graph illustrating the three regimes observed when graphene nanoribbons are heat treated using Joule heating under vacuum.

### DETAILED DESCRIPTION OF THE INVENTION

**[0010]** The invention provides a technique using chemical vapor deposition (CVD) for the bulk production (grams per day) of thin graphite ribbons consisting of long and highly crystalline nanoribbons ( $<20\text{-}30\ \mu\text{m}$  in length) exhibiting widths of  $20\text{-}300\ \text{nm}$ , and small thicknesses (2-40 layers). These layers usually exhibit ABAB . . . stacking as in highly crystalline graphite. The structure of the novel material has been carefully characterized by several techniques as well as their electronic transport and gas adsorption properties. With this material available to researchers, it is now possible to discover new applications and physico-chemical phenomena associated with layered graphene.

**[0011]** It has been shown experimentally that zigzag and armchair graphene ribbon edges result in different Raman spectra and electronic properties. For example, armchair edges result in a large intensity Raman D-band, whereas the D-band signal from zigzag edges is substantially reduced. In addition, the zigzag edges appear to have a high density of electronic states at the Fermi level.

**[0012]** Individual graphene sheets are synthesized in order to characterize Raman modes as well as physico-chemical properties. With these techniques, substrates, highly oriented pyrolytic graphite-HOPG, are used as a source of individual sheets. Unfortunately, present synthesis methods make difficult the manipulation of the nanoribbons and the amounts of sheet material is very limited. Chemical vapor deposition (CVD) is used here for producing bulk quantities of thin graphite ribbons. This material has been carefully characterized by several techniques that include: high resolution transmission electron microscopy (HRTEM), scanning electron microscopy (SEM), X-ray powder diffraction (XRD), electron diffraction (ED), X-ray photoelectron spectroscopy (XPS), thermogravimetric analyses (TGA), Raman spectroscopy, adsorption characterization, and electronic transport.

**[0013]** It is important to emphasize that a single-step and simple CVD process was used to synthesize the nanoribbons under atmospheric pressure conditions, at relatively high temperature ( $950^{\circ}\text{C}$ ). Furthermore, the physico-chemical properties of these ribbons are novel when compared with other forms of carbon. The new graphite nanoribbons material should advance the understanding of few layer graphenes, and could well be used in the fabrication of novel composites, gas storage devices, nanosensors, field emission sources, catalysts, electronic conductors, batteries, or the like.

**[0014]** The synthesis of these graphite nanoribbons was carried out using the aerosol pyrolysis process. Solutions containing 2.80 mg of ferrocene ( $\text{FeCp}_2$ ), 2.66 ml of thiophene ( $\text{C}_4\text{H}_4\text{S}$ ) in 280 ml of ethanol ( $\text{CH}_3\text{CH}_2\text{OH}$ ) were used. An aerosol was generated ultrasonically and then carried by an argon flow ( $0.8\ \text{lt}/\text{min}$ ) into a quartz tube located inside a two-furnace system heated to  $950^{\circ}\text{C}$ . (both furnaces were operated at the same temperature). After 30 minutes of operation, the ultrasonic sprayer was turned off, the Ar flow was decreased to  $0.2\text{-}0.3\ \text{lt}/\text{min}$ , and the furnaces were allowed to cool to room temperature. Once the system had cooled down, the quartz tube was removed and a black powder material was scraped from the walls of the tube located in the first furnace area.

**[0015]** The reproducibility of the experiments has been confirmed. Nevertheless, some variables were found to be critical. One of them was the storage time of the solution. It was found that 3 weeks after its preparation, the quality of the resulting thin graphene ribbon material deteriorates relative to that obtained with a fresh solution, and more by-products were produced (short nanotubes in addition to iron particles). As described above, the solution is ultrasonically vaporized, generating a dense cloud that remained constant during the 30 min synthesis period.

**[0016]** Transport measurements are carried out on individual nanoribbons inside the HRTEM and Joule heating experiments were performed that resulted in the generation of highly crystalline graphite nanoribbons. This was achieved using a HRTEM (JEOL 2010F operated at 200 keV) equipped with a scanning tunneling microscopy (STM) probe, which is further attached to a piezoelectric stage.

**[0017]** The morphology of the initial black powder consisted of ribbon-like structures exhibiting lengths of several microns, widths ranging from 100-1000 nm and thicknesses of <15 nm, as shown in FIG. 1A. It is interesting to note that the ribbons **2** revealed both flat regions as well as rippled areas, as shown in FIG. 1B. The edges of the as-prepared ribbons also displayed relatively sharp junctions that could be related to the presence of either zigzag or armchair edges, as shown in FIG. 1C. Since the ribbons were extremely thin, SEM images almost suggested transparency when observed at 10-15 keV; note the schematic of the hexagonal structure of armchair and zigzag edges underneath the HRTEM image of the ribbons depicted in FIG. 1C.

**[0018]** High-angle annular-dark-field (HAADF) images using scanning transmission electron microscopy (STEM), and dark field TEM images of the ribbons were also used to analyze the nanoribbons, respectively. The ribbons displayed only one type of contrast and Fe catalyst particles were never observed in these structures; note carbon nanotubes containing metal catalyst particles at the nanotube tips were usually produced in the second furnace while the graphene nanoribbon material was extracted from the first furnace. By performing detailed elemental energy dispersive X-ray (EDX) spectroscopy line-scans along the ribbons, it was found that the nanoribbons consisted of C, while S was notably absent. Even surface-sensitive XPS could not detect any trace of S. Although graphene nanoribbons consist of only carbon, S appears to be crucial to grow the ribbons and could well act as a catalyst.

**[0019]** In order to carry out TEM and HRTEM studies, the ribbon material (2-5 mg) was dispersed ultrasonically in methanol (10 mL) and deposited on holey carbon grids. FIG. 2A-2C depicts ribbons under TEM and HRTEM image conditions. At low magnification, the material consisted only of carbon ribbons **4** as shown in FIG. 2A. HRTEM images of the ribbons **4** are shown in FIG. 2B, which reveals the presence of hexagonal patterns **8**, that are confirmed after obtaining the fast Fourier transform (FFT) using the inset **6**. In order to confirm the graphitic structure and the layer stacking order, and to identify the edge structure, electron diffraction patterns were recorded from different ribbons as shown in FIG. 2C. Interestingly, all the ribbons we analyzed consisted of AB . . . stacked graphite, since all reflections from 3D graphite are seen in FIG. 2C, and the edges exhibited clear armchair and zigzag (or close to zigzag) morphologies after Joule heating, as shown in FIG. 1C. Heat treatment of the nanoribbons to

2800° C. increased the average L<sub>c</sub> size as shown in the inset to FIG. 3A where the narrowing of the (002) reflection is seen.

**[0020]** The average bulk structure of the ribbon materials was further studied by XRD, and it was found that the nanoribbons exhibited a highly crystalline graphite-like structure, with the presence of strong (002), (100), (101), (004) and (110) reflections as shown in FIG. 3A. It is important to note that the linewidth of the (002) diffraction line gave an average L<sub>c</sub> crystallite size of ca. 10-14 nm, in good agreement with SEM observations.

**[0021]** Raman spectroscopy measurements on the ribbons revealed the presence of the D and G bands, located at 1355 and 1584 cm<sup>-1</sup> respectively, as shown in FIG. 3B. In general, it was found that the D-band for the pristine ribbons exhibited the highest intensity, probably due to the high proportion of edges and ripples within the ribbons. Other defect sensitive Raman features were also intense. In particular, it was noted that when Raman spectra from individual ribbon edges were recorded, the presence of the D' feature at 1620 cm<sup>-1</sup>, was especially pronounced and well defined, and identified with the large number of ribbon edge structures. The disorder induced combination mode (D+G) at about 2940 cm<sup>-1</sup> is also exceptionally strong. Significant D-band intensity remained after heat treatment to 2800° C., which is identified with ribbon edges.

**[0022]** Experiments showed that the nanoribbons were highly crystalline, as suggested by TGA studies. It was found that the decomposition temperature of the ribbons in air corresponded to 702° C. for ribbons heat treated to 1000° C. in argon gas. This value is almost the same as that observed in highly crystalline carbon nanotubes produced by arc discharge techniques.

**[0023]** XPS studies revealed the nature of the carbon bonds present in the sample. The material contained sp<sup>2</sup> and sp<sup>3</sup> hybridized carbon atoms (39% sp<sup>2</sup> and 39% sp<sup>3</sup>), and the rest of the carbonaceous material was bonded to O and consisted of carbonyl groups (C=O) and carboxylic groups (COO); note that 85 at % corresponded to C and 15 at % to O. It is understood that the large number of sp<sup>3</sup> hybridized carbon atoms was caused by the exposed edges and the rippled (highly curved) regions within the nanoribbons. The 1:1 ratio of sp<sup>3</sup>:sp<sup>2</sup> carbon atoms could also explain the large intensity of the D-band observed in Raman spectroscopy, because the material was indeed highly crystalline and showing an AB . . . stacking of the graphene layers.

**[0024]** N<sub>2</sub> adsorption measurements on the carbon nanoribbons revealed a BET surface area of 59 m<sup>2</sup>/g, which was similar to the surface area of acetylene black (86 m<sup>2</sup>/g). The adsorption data indicated that the nanoribbon material corresponds to a flat surface, which was not porous to N<sub>2</sub> molecules. The interaction of an N<sub>2</sub> molecule with the surface of the nanoribbon is weaker than that with well-crystalline carbon black, which is in agreement with the presence of predominant edge-like surfaces. However, H<sub>2</sub> adsorption at 77 K indicated the presence of rather strong sites for supercritical H<sub>2</sub> adsorption corresponding to ca. 15 % of the monolayer capacity of N<sub>2</sub>. Consequently, the nanoribbon should have a unique nanostructural fit for the adsorption of supercritical H<sub>2</sub>.

**[0025]** In order to study electron transport along these nanoribbons, in-situ transport measurements using a piezo stage inside a HRTEM were carried out. Two electrodes **12**, **14** were attached to a piece of an individual ribbon **10**, and a voltage started to be applied across the ribbon, as shown in FIG. 4A.

Subsequently, I-V curves for different ribbons, before and after annealing by Joule heating, are shown in FIGS. 4B. For all ribbons studied, the material behaved like a metal that followed Ohm's law. For the ribbon shown in FIG. 4A, a 20 k $\Omega$  resistance value was measured when a low voltage was applied. Interestingly, after a voltage of 1.6 V was applied for more than 15 minutes, the resistance value dropped to 10.5 k $\Omega$ , corresponding to the structure 20 shown in FIG. 4C, suggesting that crystallization of the material due to Joule heating had taken place.

[0026] These results shown in FIG. 4B confirm that the ribbons behave like metals. Specifically, FIG. 4D reveals the exceptional clarity of the many long zigzag and armchair edges that are usually observed after the Joule heating is applied. Here, one can clearly see that the ribbon edge could be commensurate with armchair and zigzag orientations. In addition, the FFT from FIG. 4D (shown in the inset to FIG. 4C) confirms the AB layer stacking of the graphene ribbon.

[0027] Due to the large proportion of edges, it is possible that the edges could emit electrons when a voltage is applied. In particular, anodes containing graphene nanoribbons could be used as electron field emission sources.

[0028] These ribbons could also be exfoliated (detachment of the layers into individual layers) and cut into shorter pieces and into narrow ribbons. The exfoliation process usually consists in intercalating atoms or molecules (e.g. Li, K, H<sub>2</sub>SO<sub>4</sub>, FeCl<sub>3</sub>, Br<sub>2</sub>, etc) between layers, followed by rapid reactions in liquids or by subjecting the material to abrupt temperature changes. It is therefore clear that the exfoliated form of these ribbons (containing several exposed edges) could be used as gas storage devices, electronic wires, sensors, catalytic substrates, etc. By using this material, it is now possible to unveil new applications and novel physico-chemical properties associated with layered sp<sup>2</sup> hybridized carbon.

[0029] It is also possible to dope these ribbons with N, P, B, Si and other elements. By doping, the physicochemical properties of these ribbons are modified. For example, the presence of substitutional atoms in the hexagonal carbon lattice could make more reactive sites that will also modify the electronic properties as well as the electrical and thermal conductivity of the nanoribbons.

[0030] The structures produced using the invention could also be heat treated under an inert gas like argon (FIGS. 3A and 3B) and then further modified under vacuum using Joule heating by applying a voltage across the length of the nanoribbon to cause current flow. Heating by this dynamic process dramatically increases the crystallinity and establishes interplanar AB stacking order and well-defined graphene edges, principally along the zigzag edges. The new material thus formed has its own distinct properties depending on both the static heat treatment conditions (FIG. 3) and the Joule heating conditions (FIG. 4). Further control of these structures can be achieved by combining the heat treatment procedure with Joule heating described herein in varying proportions.

[0031] FIG. 5 shows three regimes of behavior used in Joule heating: low Joule heating (Regime 1), where the current follows the applied voltage linearly. In Regime 2, annealing by Joule heating results in a dramatic improvement in crystallinity. The mechanism responsible for the observed increase in crystallinity is identified with an electro-migration process which serves to anneal defects was discussed herein. Beyond some value of the applied voltage, the temperature of the ribbon gets too high and the breakdown of graphene layers starts, defining the onset of Regime 3. In this regime, layers of

graphene continue to vaporize and eventually some weak link along the ribbon fractures causing an open circuit.

[0032] The invention allows for the first time to synthesize bulk amounts of a novel form of nanocarbon (graphene nanoribbons). This material was characterized using diverse techniques and the results have confirmed that graphene nanoribbons are indeed a promising novel nanocarbon form of carbon which could be interesting for both scientific studies of graphene edges and for practical applications. It is possible that in the future, these ribbons could be exfoliated into individual graphene sheets providing new possibilities for detailed studies of the structure and properties of clean graphene edges, not previously available. The ribbons could also be used to attach metal particles and other biological molecules on the surface and at the edges, and therefore they could be used as sensors, and protein immobilizers. The ribbon material could also be used to incorporate Li-ions in between the graphene layers so as to store the Li ions. This behavior is important in the fabrication of Li-ion batteries, in which the anodes would contain graphene nanoribbons.

[0033] Although the present invention has been shown and described with respect to several preferred embodiments thereof, various changes, omissions and additions to the form and detail thereof, may be made therein, without departing from the spirit and scope of the invention.

What is claimed is:

1. A method of forming bulk nanoribbon structure comprising:
  - forming a plurality of thin graphite ribbons having long and highly crystalline nanoribbons; and
  - annealing said thin graphite ribbons using Joule heating by applying a voltage across the length of the thin graphite ribbons to cause current flow so as to produce heat that increases crystallinity as well as establishing interplanar stacking order and well-defined graphene edges of said thin graphite ribbons.
2. The method of claim 1, wherein thin graphite ribbons attach to metal particles and other biological molecules on the surface.
3. The method of claim 1, wherein thin graphite ribbons comprises N, P, B, Si as dopants.
4. The method of claim 1, wherein thin graphite ribbons comprises Li-ions as dopants.
5. The method of claim 1, wherein said graphene edges emit electrons when a voltage is applied
6. The method of claim 1, wherein said thin graphite ribbons are exfoliated using Li, K, H<sub>2</sub>SO<sub>4</sub>, FeCl<sub>3</sub>, Br<sub>2</sub>.
7. The method of claim 1, wherein said highly crystalline nanoribbons comprise a length less than 30  $\mu$ m.
8. The method of claim 7, wherein said highly crystalline nanoribbons comprise a width between 20 nm and 300 nm.
9. The method of claim 1, wherein said interplanar stacking order comprises an ABAB . . . stacking order.
10. The method of claim 1 further comprising treating said thin graphite ribbons in an Argon flow at high temperatures up to 2800° C. using a graphite oven.
11. A bulk nanoribbon structure comprising a plurality of thin graphite ribbons having long and highly crystalline nanoribbons, wherein a voltage is applied across the length of the thin graphite ribbons to cause current flow so as to increase crystallinity as well as establishing interplanar stacking order

and well-defined graphene edges of said thin graphite ribbons.

**12.** The bulk nanoribbon structure of claim **11**, wherein thin graphite ribbons attach to metal particles and other biological molecules on the ribbon surface.

**13.** The bulk nanoribbon structure of claim **11**, wherein thin graphite ribbons comprises N, P, B, Si as dopants.

**14.** The bulk nanoribbon structure of claim **11**, wherein thin graphite ribbons comprises Li-ions as dopants.

**15.** The bulk nanoribbon structure of claim **11**, wherein said graphene edges emit electrons when a voltage is applied

**16.** The bulk nanoribbon structure of claim **11**, wherein said thin graphite ribbons are exfoliated using Li, K, H<sub>2</sub>SO<sub>4</sub>, FeCl<sub>3</sub>, Br<sub>2</sub>.

**17.** The bulk nanoribbon structure of claim **11**, wherein said highly crystalline ribbons comprise a length less than 30  $\mu\text{m}$ .

**18.** The bulk nanoribbon structure of claim **17**, wherein said highly crystalline nanoribbons comprise a width between 20 nm and 300 nm.

**19.** The bulk nanoribbon structure of claim **11**, wherein said interplanar stacking order comprises an ABAB . . . stacking order.

**20.** The bulk nanoribbon structure of claim **17**, said thin graphite ribbons are treated in an Argon flow at high temperatures up to 2800° C. using a graphite oven to modify original properties.

\* \* \* \* \*